12TH INTERNATIONAL KIMBERLITE CONFERENCE
12 IKC
30 YEARS OF DIAMONDS IN CANADA
8–12 July 2024 • Yellowknife
12th International Kimberlite Conference Extended Abstract No. 12IKC-115, 2024

Dynamical properties of defects in diamond

Razvan Caracas
Institut de Physique du Gobe de Paris, CNRS, Université Paris Cité,
1 rue Jussieu 75005, Paris, France; caracas@ipgp.fr
and
Center for Planetary Habitability (PHAB), University of Oslo,
Oslo, Norway; Razvan.caracas@geo.uio.no

Introduction

First, we compute the theoretical Raman spectra of various diamond polymorphs to help provide a quick, non-destructive method of determining planar defects in diamonds.

For this, we use density functional perturbation theory and compute the Raman spectra with peak position and intensity [1-5]. In density functional perturbation theory, the electronic energy F of an atomic ensemble is expanded as a Taylor series around the equilibrium position of the atoms, with respect to a series of perturbations λ acting along directions i,j,k .. :

$$F_{e+i}[\lambda] = F_{e+i}^{(0)}[\lambda] + \sum_i \left(\frac{\partial F_{e+i}}{\partial \lambda_i}\right)\lambda_i + \frac{1}{2}\sum_{ij}\left(\frac{\partial^2 F_{e+i}}{\partial \lambda_i \partial \lambda_j}\right)\lambda_i\lambda_j + \frac{1}{6}\sum_{ij}\left(\frac{\partial^3 F_{e+i}}{\partial \lambda_i \partial \lambda_j \partial \lambda_k}\right)\lambda_i\lambda_j\lambda_k + \ldots$$

The Raman spectra involve atomic displacements and electric fields as perturbations. The Raman tensor, α, determines the intensity of the Raman spectra. Its components are obtained as:

$$\alpha_{ij}^{m} = \sqrt{\Omega_0}\sum_{\kappa\beta}\frac{\partial \chi_{ij}^{\infty(1)}}{\partial \tau_{\kappa\beta}}\eta_m(\kappa\beta) = \sqrt{\Omega_0}\sum_{\kappa\beta}\frac{\partial}{\partial \tau_{\kappa\beta}}\left(\frac{\partial^2 E}{\partial \mathcal{E}_i \partial \mathcal{E}_j}\right)\mathcal{E}_i\mathcal{E}_j\eta_m(\kappa\beta)$$

where τ are displacements of atoms β along directions κ, χ is the dielectric tensor, *i, j, m* are cartesian directions, and $\mathcal{E}$ are electric fields.

Here, we use the ABINIT implementation of the DFPT. Simulations are performed using the Local Density Approximation for the exchange-correlation factor. Results are reported in Figure 1. All the details of the simulations, as well as the raw spectra, can be found on the WURM website [6]. Most of the diamond polytypes are hexagonal; they are all obtained from a different packing sequence. Their occurrence in natural or synthetic diamonds may result as growth defects [7].

All the spectra are dominated by the characteristic T3g peak of diamond at 1303 cm^{-1}. Note that the theoretical spectrum was realized using an 8x8x8 grid of special k points; this ensured an error of only 1 cm^{-1} with respect to experimental data. The spectra were obtained at the experimental density, the slightest change in volume greatly affecting the position of the peaks [8].

While it is hard to distinguish between various individual hexagonal polytypes, their presence can be observed by the appearance of extra peaks and shoulders [9]. The main characteristic of the other polytypes, except for the pure 3C diamond, is the presence of various smaller shoulder peaks in the 1200 – 1300 cm^{-1} range. As the succession of sp3 bonds of carbon is interrupted, the symmetry is broken, resulting in the activation of certain phonons observed in the new Brillouin zones. Further supplementary peaks may occur at low frequency, in the 300 – 600 cm^{-1} range.

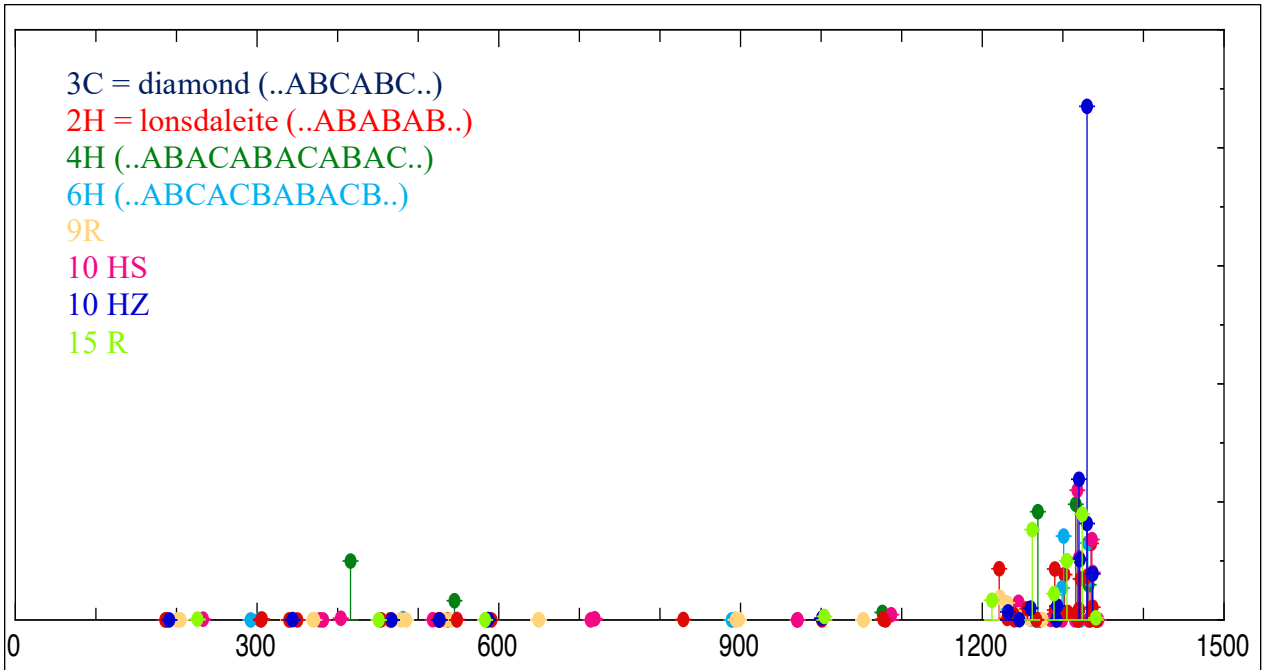

Figure 1. Raman spectra of various diamond polymorphs. All spectra are dominated by the main, typical T3g peak of the diamond at 1303 cm^{-1}.

In a second set of simulations, I study the diffusion of Helium in diamond. For this, we employ molecular dynamics (MD) simulations in the Vienna Ab Initio Simulation package [10,11]. I use density functional theory to generate a series of reference structures and MD trajectories. Then, I use machine learning techniques to fit interatomic potentials on the ab initio data. To ensure the quality of the potentials and to avoid unphysical structures, I also generate a series of configurations characterized by very large interatomic forces and high energies. As I study the diffusion of He in diamond along a mantle adiabat, I refine the machine learning potentials at each pressure.

With the machine-learning potentials, I use large simulation boxes with 1728 atoms, corresponding to 6x6x6 supercells of the conventional Fm3m unit cell of diamond, in which I randomly insert one He atom. The simulations are run with a time step of 0.5 femtosecond. After a thermalization period of 1000 steps, the simulations record a production length of 400 to 600 picoseconds. I employ the Universal Molecular Dynamics package [12] to perform the post-processing analysis of the MD runs.

I report the diffusion coefficients as a function of pressure and temperature, following the mantel geotherm. I find that temperature is the major factor ruling the diffusion coefficients of He in diamonds.

References

1. Baroni, S., de Gironcoli, S., Dal Corso, A., and Giannozzi, P. (2001) Phonons and related crystal properties from density-functional perturbation theory. Review of Modern Physics, 73, 515–562.
2. X. Gonze, G.-M. Rignanese, M. Verstraete, J.-M. Beuken, Y. Pouillon, R. Caracas, F. Jollet, M. Torrent, et al. (2005) A brief introduction to the ABINIT software package. Zeitschrift für Kristallographie, 220, 558–562.

3. X. Gonze, G.-M. Rignanese and R. Caracas (2005) First-principles studies of the lattice dynamics of crystals, and related properties. Zeitschrift für Kristallographie, 220, 458–472.
4. R. Caracas, and X. Gonze (2010) Lattice dynamics and thermodynamical properties. In Chaplot, S.L., Mittal, R., and Choudhury, N., Eds., Thermodynamic Properties of Solids: Experiment and Modeling, p. 291–315. Wiley-VCH Verlag, Weinheim.
5. Baroni, S. and Resta, R. (1986) Ab initio calculation of the low-frequency Raman cross section in silicon, Physical Review B, 33, 5969–5971.
6. R. Caracas, E. Bobocioiu (2011) The WURM project—a freely available web-based repository of computed physical data for minerals. American Mineralogist 96, 437-443
7. Z Wang, Y Zhao, C Zha, Q Xue, RT Downs, RG Duan, R Caracas, X Liao (2008) X-Ray Induced Synthesis of 8H Diamond. Advanced Materials 20, 3303-3307
8. N Dubrovinskaia, L Dubrovinsky, R Caracas, M Hanfland (2010) Diamond as a high pressure gauge up to 2.7 Mbar. Applied Physics Letters 97 (25)
9. D. C. Smith, G. Godard (2009) UV and VIS Raman spectra of natural lonsdaleites: Towards a recognised standard. Spectrochimica Acta Part A: Molecular and Biomolecular Spectroscopy, 73, 428-435
10. G. Kresse, J. Furthmuller (1996) Efficiency of ab-initio total energy calculations for metals and semiconductors using a plane-wave basis set, Computational materials science 6, 15–50.
11. P. E. Blochl (1994) Projector augmented-wave method, Physical Review B 50, 17953.
12. R. Caracas, A. Kobsch, N. V. Solomatova, Z. Li, F. Soubiran, J.-A. Hernandez (2021) Analyzing melts and fluids from ab initio molecular dynamics simulations with the UMD package, JoVE (Journal of Visualized Experiments), e61534